

See discussions, stats, and author profiles for this publication at: <https://www.researchgate.net/publication/231271056>

# Structural Analysis of Soluble and Insoluble Fractions of Asphaltenes Isolated Using the PNP Method. Relation between Asphaltene Structure and Solubility

ARTICLE *in* ENERGY & FUELS · DECEMBER 2003

Impact Factor: 2.79 · DOI: 10.1021/ef030065y

---

CITATIONS

30

---

READS

27

## 5 AUTHORS, INCLUDING:



Socrates Acevedo

Central University of Venezuela

111 PUBLICATIONS 1,269 CITATIONS

[SEE PROFILE](#)

# Structural Analysis of Soluble and Insoluble Fractions of Asphaltenes Isolated Using the PNP Method. Relation between Asphaltene Structure and Solubility

Sócrates Acevedo,<sup>\*,†</sup> Optalí Escobar,<sup>†</sup> Lorenzo Echevarría,<sup>‡</sup>  
Luis B. Gutiérrez,<sup>†</sup> and Bernardo Méndez<sup>§</sup>

Laboratorio de Fisicoquímica de Hidrocarburos, Laboratorio de Espectroscopía Laser,<sup>‡</sup> Laboratorio de Resonancia Magnética Nuclear, Universidad Central de Venezuela,  
Facultad de Ciencias, Escuela de Química. 47102, Caracas 1041, Venezuela

Received March 20, 2003. Revised Manuscript Received October 27, 2003

Both, the toluene-insoluble (A1) and toluene-soluble (A2) asphaltene fractions, isolated using the PNP method, have been characterized by elemental analysis, molecular weight (VPO, SEC, and LDMS), and NMR (<sup>1</sup>H and <sup>13</sup>C). The most prominent results of the analysis were the differences in hydrogen aromaticity  $f_H$ , high content in both fractions of hydrogen bonded to aliphatic carbons joined to aromatics ( $f_a$ ), and differences in carbon aromaticity  $f_c$ . Thus, low  $f_H$  and high  $f_a$  in A1 were consistent with a single, rigid, and flat core formed by fusion of polycyclic aromatic and naphthenic units (a single and large PANU), whereas for A2, high  $f_H$  and high  $f_a$  were consistent with a more flexible structure where several smaller PANU are joined by aliphatic chains. Using a MM program, models for A1 and A2 were built and the solubility parameters calculated were found in keeping with solubility difference suggesting that the above structural differences account for the solubility difference. Similar molecular weight and heteroatom content found for these fractions suggest that these play a minor or insignificant role in solubility. A dispersion mechanism of A1 by A2, relevant to solubility of asphaltene in organic solvents, is proposed.

## Introduction

Due to asphaltenes significant and mainly negative impact on the petroleum industry, studies in their colloidal<sup>1,2</sup> and molecular<sup>3–17</sup> properties have been and

continue to be very active and important research topics. In particular, asphaltene molecular structure is an interesting but extremely difficult area that has been the subject of many studies.<sup>3–17</sup> These studies have made a very important contribution to our present knowledge of asphaltene structure.

There is no doubt that progress in structure determination would benefit a lot from fractionation of the mixture. However, asphaltene fractionation is not an obvious choice. Fractionation of asphaltenes by chromatography<sup>6</sup> and other means<sup>11,18</sup> has been attempted many times. However, due to factors such as chemisorption and precipitation, typical adsorption chromatography of asphaltenes on mineral surfaces such as silica or alumina is unreliable to say the least. For instance, it is known that silica and other active adsorption solids promote asphaltene precipitation.<sup>19</sup> Thus, poor fractionation should be expected for asphalt-

- \* Corresponding author. E-mail: soaceved@strix.ciens.ucv.ve.  
† Laboratorio de Fisicoquímica de Hidrocarburos.  
‡ Laboratorio de Espectroscopía Laser.  
§ Laboratorio de Resonancia Magnética Nuclear.  
(1) Sheu, E. Y.; Storm, D. A. *Asphaltenes: Fundamentals and Applications*; Sheu, E. Y., Mullins, O. C., Eds.; Plenum Press: New York, 1995; Chapter 1, p 1.  
(2) Acevedo, S.; Ranaudo, M. A.; Escobar, G.; Gutiérrez, L. B.; Gutiérrez, X. *Asphaltenes: Fundamentals and Applications*; Sheu, E. Y., Mullins, O. C., Eds.; Plenum Press: New York, 1995; Chapter 4, p 131.  
(3) Speight, J. G.; Moschopedis, S. *Chemistry of Asphaltenes*; Bunker, J. W., Li, N. C., Eds.; Advances in Chemistry Series, 195. American Chemical Society: Washington, DC, 1981; Chapter 1, p 1.  
(4) Long, R. B. *Chemistry of Asphaltenes*; Bunker, J. W., Li, N. C., Eds.; Advances in Chemistry Series, 195. American Chemical Society, Washington, DC, 1981; Chapter 2, p 17.  
(5) Yen, T. F. *Chemistry of Asphaltenes*; Bunker, J. W., Li, N. C., Eds.; Advances in Chemistry Series, 195. American Chemical Society: Washington, DC, 1981; Chapter 4, p 39.  
(6) Selucky, M. L.; Kim, S. S.; Skinner, F.; Strausz, O. P. *Chemistry of Asphaltenes*; Bunker, J. W., Li, N. C., Eds.; Advances in Chemistry Series, 195. American Chemical Society, Washington, DC, 1981; Chapter 6, p 83.  
(7) Boduszynsky, M. W. *Chemistry of Asphaltenes*; Bunker, J. W., Li, N. C., Eds.; Advances in Chemistry Series, 195. American Chemical Society: Washington, DC, 1981; Chapter 7, p 119.  
(8) Speight, J. G. *The Chemistry and Technology of Asphaltenes*, 3rd ed.; Marcel Dekker Inc.: New York, 1999; Chapter 10, p 453.  
(9) Mullins, O. C. *Asphaltenes: Fundamentals and Applications*; Sheu, E. Y., Mullins, O. C., Eds.; Plenum Press: New York, 1995; Chapter 2, p 53.  
(10) Ignasiak, T.; Kemp-Jones, A. V.; Strausz, O. P. *J. Org. Chem.* **1977**, *42*, 312–320.

- (11) Semple, K. M.; Cir, N.; Fedorak, P. M.; Westlake, D. W. S. *Can. J. Chem.* **1990**, *68*, 1092.  
(12) Payzant, J. D.; Lown, E.; Strausz, O. P. *Energy Fuels* **1991**, *5*, 445–453.  
(13) Platanov, V. V.; Proskuryakov, V. A.; Klyavina, O. A.; Klibabina, N. A. *Russ. J. Appl. Chem.* **1994**, *67*, 440–443.  
(14) Storm, D. A.; Sheu, E. Y.; Detar, M. M.; Barresi, R. J. *Energy Fuels* **1994**, *8*, 567–569.  
(15) Peng, P.; Morales-Izquierdo, A.; Hogg, A.; Strausz, O. P. *Energy Fuels* **1997**, *11*, 1171–1187.  
(16) Miller, J. T.; Fisher, R. B.; Thiagarajam, P.; Winans, R. E.; Hunt, J. E. *Energy Fuels* **1998**, *12*, 1290–1298.  
(17) Strausz, O. P.; Mojelsky, T. W.; Lown, E. *Energy Fuels* **1999**, *13*, 228–247.  
(18) Yang, M.; Esser, S. *Prepr. Pap.—Am. Chem. Soc., Div. Fuel Chem.* **1999**, *44* (4), 768.

enes in adsorption chromatography. Although other methods such as preparative SEC have been employed,<sup>11</sup> their use as routine methods is questionable. For instance, even under analytical conditions, asphaltene SEC usually affords a single broad band with little or no evidence of resolution.<sup>20</sup>

Due to the extreme complexity of asphaltene mixtures, usual solvent fractionation with solvent mixtures leads to a fraction series where properties change slowly in a continuous manner, complicating the analysis and interpretation.

In a recent paper, a new separation method, hereafter called the "PNP method", was reported<sup>21</sup> (see below). Clean fractionation into two very different fractions A1 (about 70%) and A2 (about 30%) was achieved with this method. The most important result reported in this paper was the very large solubility difference found for A1 and A2. Solubility values for Furrial asphaltenes and fractions A1 and A2 were, respectively, 56, 0.09, and 57 g/L in toluene at room temperature. Thus, use of the PNP method could lead to important information regarding the role of fractions in the mixture. For instance, despite the large toluene solubility of the complete mixture, this contains a major component which is practically insoluble. This result is consistent with the colloidal nature of asphaltenes where A1 occupies the colloidal insoluble core and A2 the soluble periphery.<sup>21</sup>

Although dispersion of A1 by A2 is consistent with the formation and dispersion of asphaltene colloids in toluene,<sup>1</sup> the mechanism for this process and the structural features responsible for the solubility difference are unknown.

The emphasis in this paper is on the characterization of fractions A1 and A2 and in the proposition of general structural features that could be useful to account for their solubility difference. It should be realized that even for relatively simple molecules, solubility behavior is difficult to predict since too many factors enter the picture. Fortunately, as shown below, very significant differences and similarities were found in the NMR spectra of these fractions from which general structural information could be obtained.

For the purpose of analyzing and discussing the results, using a simple but plausible approach, models representing the above fractions were constructed where several polycyclic aromatic and naphthenic units or PANU modeled the structure. When these were fused together, leading to a rigid and flat core structure, represented by a single and large PANU, a relatively high solubility parameter  $\delta$ , consistent with low solubility and other properties found for A1, was calculated using a MM program. On the other hand, when aliphatic chains connect smaller PANU, leading to a more flexible structure, a relatively low  $\delta$  value, in keeping with the high solubility and other properties of A2, was calculated.

On the basis of the  $M_w$  measurements of this paper and the discussion below, a mechanism for dispersion

of A1 by A2 is proposed whereby presence of A2 in the solid mixture leads to a loosely packed solid promoting its dispersion.

## Experimental and Methods

Furrial asphaltenes were obtained from the crude oil (20° API) as described earlier.<sup>21</sup> The usual addition to the crude of 60 *n*-heptane volumes, followed by filtration, Soxhlet extraction to remove resins, and vacuum treatment was employed.

Fractions A1 and A2 were obtained by mixing an asphaltene cumene solution with a saturated solution of PNP in cumene using a modification of the method described.<sup>21</sup> Here the asphaltene solution was 2 g L<sup>-1</sup>. Precipitated solid composed of A1 and PNP was collected after 3 days, filtered, washed with toluene, dried, dissolved in chloroform, and the PNP was extracted repeatedly with an aqueous solution of NaOH. Extraction was monitored by TLC-FID using the following solvent sequence: heptane, toluene, dichloromethane, and dichloromethane-methanol. Here a yellow band could be easily separated whenever the phenol was present. Yield: 50% of A1 after evaporation of chloroform in a vacuum. The filtrate from the above filtration was evaporated to dryness under vacuum, dissolved in chloroform, and treated as described for A1 to remove PNP. The solid obtained was redissolved in cumene, treated with a saturated solution of picric acid (2,4,6-trinitrophenol), and the above procedure was applied to obtain an additional 20% of A1 and a 30% yield of A2.

Elemental analysis (CHN) was measured in a Perkin-Elmer equipment model 2400. Sulfur was measured in IRIS Thermo Jarrel Ash plasma equipment. Double-bond equivalents (double bonds plus rings) were calculated using eq 1, where C, H, and N represent the number of these atoms per hundred carbons atoms.

$$\text{DBE} = \frac{202 + N - H}{2} \quad (1)$$

**Molecular Weight.** VPO molecular weight measurements were determined in nitrobenzene at 100 °C using pyrene as calibration standard. Four or more solutions were measured in the 1 to 4 g L<sup>-1</sup> concentration range, and the linear plots (negative slopes) were extrapolated to zero concentration to obtain the number average molecular weight  $M_n$ .

SEC molecular weights were obtained using THF as the mobile phase and a UV detector as described earlier.<sup>20</sup> When required, the definition of  $M_n$  (eq 2) was used to obtain a calculated value for mixtures of A1 and A2.

$$M_n = \frac{m}{\frac{m_1}{M_{n1}} + \frac{m_2}{M_{n2}}} \quad (2)$$

In this equation,  $m$ ,  $m_1$ , and  $m_2$  represent masses of the mixture and components whereas the  $M_{n1}$  are the respective  $M_n$  values.

LDMS mass spectra were acquired on a PerSeptive Biosystems Voyager-DE STR mass spectrometer using 337 nm light from a pulsed nitrogen laser for ionization. Samples were prepared by dissolving approximately 50 µg of material in 500 µL of THF. Aliquots of 0.5 µL were deposited on the gold-plated target, and the solvent was evaporated under ambient laboratory conditions. Samples were analyzed as soon as possible to minimize evaporation of more volatile components. Ionization was conducted using a laser setting slightly above the threshold for ionization. A total of 256 laser shots were acquired over numerous sites within each sample.

**Molecular Models.** 3D molecular models were calculated using a (MM+) molecular mechanics program of HyperChem. Unless stated otherwise, energy differences for dimers and trimers were calculated for local minima corresponding to co-

(19) Castillo, J.; Fernández, A.; Ranaudo, M. A.; Acevedo, S. *Pet. Sci. Technol.* **2001**, *19*, 79–110.

(20) Acevedo, S.; Escobar, G.; Ranaudo, M. A.; Rizzo, A. *Fuel* **1998**, *77*, 853.

(21) Gutiérrez, L. B.; Ranaudo, M. A.; Méndez, B.; Acevedo, S. *Energy Fuels* **2001**, *15*, 624–628.

**Table 1. Elemental Analysis and Other Properties of Samples Studied**

sample	percentage	C	H	N	S	O <sup>a</sup>	H/C	N/C	S/C	O/C	DBE
asphaltene	5 <sup>c</sup>	85.27	6.99	2.10	3.4	2.5	0.98	0.021	0.015	0.022	53
A1 <sup>b</sup>	70 <sup>d</sup>	83.56	6.45	2.32			0.92	0.024			56
A2 <sup>b</sup>	30 <sup>d</sup>	83.19	7.08	2.11			1.02	0.021			51

<sup>a</sup> By difference. <sup>b</sup> Fractions from furrial asphaltenes. <sup>c</sup> Respect crude oil. <sup>d</sup> Respect asphaltene.

facial superposition. Molecular volumes  $V$  of optimized structures were estimated using the Periodic Box sub-routine of HyperChem. This simple calculation was performed by taking  $V$  equal to the number of water molecules displaced from a box filled with water after placing the solute within the box. For this purpose we use eq 3:

$$V = (n_0 - n)18.015 \quad (3)$$

Here  $V$  is in cubic centimeters (cc), 18.015 is the molar volume of water assuming a density equal to one and  $n_0$  and  $n$  are, respectively, the maximum number of water molecules in a cubic box before and after placing the solute within the box. For convenience, the smallest box enclosing solute was selected. The recommended minimum distance (2.3 Å) between water and solute was used.

Model building for A1 and A2 was assisted by the experimental results in this paper. The size of molecules was estimated using the VPO  $M_n$  value of samples, and the number of carbons and hydrogens was estimated from the H/C ratio. The NMR information was used to divide these atoms in aromatic and aliphatic and to estimate the number of aliphatic carbons in rings and chains. Energies of models correspond to local minima. For simplicity, only one atom of each heteroatom (N, O, and S) was included in these models.

Solubility parameter values  $\delta$  were calculated using eq 4, where  $\Delta E$  (always negative) is the MM+ energy of dimer or trimer formation.

$$\delta = \left( \frac{-\Delta E}{V} \right)^{1/2} \quad (4)$$

**NMR.** NMR spectra were recorded on a JEOL EX 270 Fourier transform NMR spectrometer using CD<sub>2</sub>Cl<sub>2</sub>; tetramethylsilane was used as an internal standard. The instrument was equipped with a 5 mm broadband probe head. Processing were performed using the program DELTA V1.8 running on a Silicon Graphics Workstation. The selected parameters were as follows: spectral window, 250 ppm; width of 30° pulses, 2.8  $\mu$ s; relaxation delay, 5 s; and number of scans, 8000–12000. The spectra were obtained using standard JEOL software.

## Results

Table 1 shows elemental analysis and other properties of samples studied. Besides H/C, DBE is a useful parameter related to the number of double bonds and rings in these samples. For instance, it could be shown that for any reasonable structure consistent with experimental results, the aromatic units cannot account for all DBE. This means that a significant number of aliphatic or naphthenic rings must be included. Comparison of nitrogen and oxygen content (Table 1) and solubility (Table 2) corresponding to asphaltene samples shows that heteroatom content does not play a major role in solubility.

Significant differences in both  $f_H$  and  $f_C$  were found for fractions A1 and A2 (see Table 3 and Figures 1 and 2). As shown in the <sup>1</sup>H spectra of Figure 1, significant  $f_a$  values (see Table 4) corresponding to methyl, methylenic ( $-CH_2-$ ), and methynic ( $-CHR-$ ) hydrogens,

**Table 2. NMR and Solubility Properties**

sample	$f_C^a$	$f_H^b$	$f_{H_a}^c$	solubility <sup>d</sup> (g/L)
asphaltene	49	20	14	57
A1	63	8	31	0.09
A2	55	22	30	56

<sup>a</sup> Percentage of aromatic carbons. <sup>b</sup> Percentage of aromatic hydrogen. <sup>c</sup> Percentage of  $H_a$ -type hydrogens (approximated values). <sup>d</sup> From ref 21; in toluene, room temperature.

**Table 3.  $M_n$  Values for Furrial Samples**

sample	VPO <sup>a</sup>	SEC <sup>b</sup>	LDMS <sup>c</sup>
asphaltenes	980 (1554) <sup>d</sup>	2600 (2830) <sup>d</sup>	1400
A1	2600	3000	1400
A2	970	2200	1400

<sup>a</sup> In nitrobenzene at 100 °C. <sup>b</sup> THF mobile phase. <sup>c</sup> See text.

<sup>d</sup> Calculated using eq 2, composition in Table 1 and VPO values in this table.

bonded to aromatic carbons (here generally refer to as  $H_a$ ), extending from 1.8 to 3.35 ppm approximately, were found for A1 and A2. In other words, these chemical shifts correspond to hydrogen in bonds such as Ar—CH—. Since in this range (1.8 to 3.35, see Figure 1) extensive band superposition is apparent, the  $f_a$  values shown in Table 3 are approximated.

For comparison, molecular weights of fractions A1 and A2 were measured by several techniques and the results are shown in Table 3. In other words, we are not interested in any particular value given by any particular technique but in the difference between A1 and A2 measured using any one of these techniques.

LDMS afforded the same values for A1 and A2, suggesting that  $M_w$  is not a major factor for solubility difference. Accordingly, a small difference was measured by SEC.

When compared to LDMS and SEC, a rather large  $M_n$  difference was measured by VPO. This difference, and the fact that asphaltene mixture yields a value similar to A2, is probably due to A1 aggregation (see below).

For asphaltenes mixtures, and using eq 1,  $M_n$  values could be calculated assuming that the mixture is made of A1 and A2 with the composition shown in Table 1. The results of these calculations are shown in Table 3. It is noteworthy that whereas for the SEC case the calculated and experimental values are very close to each other, a very large difference was found for the VPO case.

To assist the present discussion we have built the models shown in Figure 3 for A1 and A2. Table 4 shows a comparison of the structural features of models with the present experimental data. In building these models, we use the experimental results of this work as much as possible. Number of carbons and hydrogens was adjusted to keep the  $M_w$  close to the experimental  $M_n$  for A2 (970, VPO). As mentioned above, it is important to note that according to the <sup>1</sup>H NMR spectra (see Figure 1) these fractions contain significant quantities

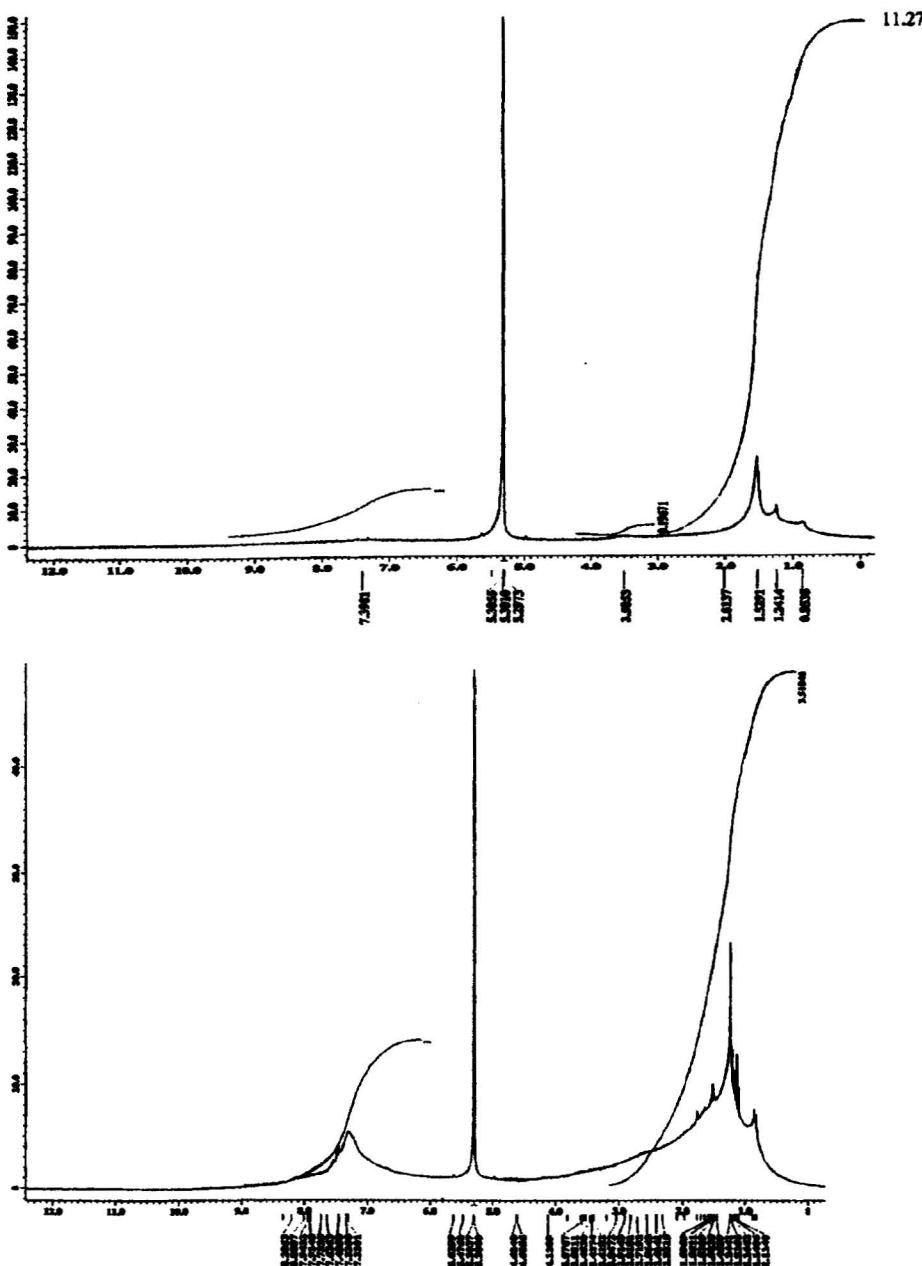


**Figure 1.** <sup>1</sup>H NMR spectra of fractions A1 (top) and A2 (bottom). In CD<sub>2</sub>Cl<sub>2</sub>, room temperature.

of  $H_o$  hydrogen (high  $f_o$ ). This could be accounted for (see below) both in terms of naphthenic rings fused to aromatic rings and/or in terms of aliphatic chains joined to aromatics. This, combined with the low  $f_H$  and high  $f_C$  for A1, suggests fusion of aliphatic and aromatic rings leading to a core formed by polycyclic aromatic and naphthenic units (PANU) fused in a single, large, and mainly flat PANU, such as the one shown in Figure 3a.

On the other hand, for A2, high  $f_H$  combined with high  $f_C$  and high  $f_o$  means low substitution for peripheral aromatic carbons, and suggests the presence of several smaller PANU joined by aliphatic chains. This information was used for building Model 2 of Figure 3b.

Although guided by general knowledge of asphaltene structure, other aspects such as heteroatom position and functionalities, ring size and position, and chain position are arbitrary. For comparison purposes, energies for models and other aggregates are shown in Table 5. For dimers and trimers, energies values were calculated after placing the molecules on top of each other (co-facial superposition). These values correspond to local minima, and no search for global minima was performed.

Solubility parameters were calculated using eq 4. Values for models A1 and A2 are shown in Table 5. Plausibility of this equation was examined by comparison with experimental values reported for several

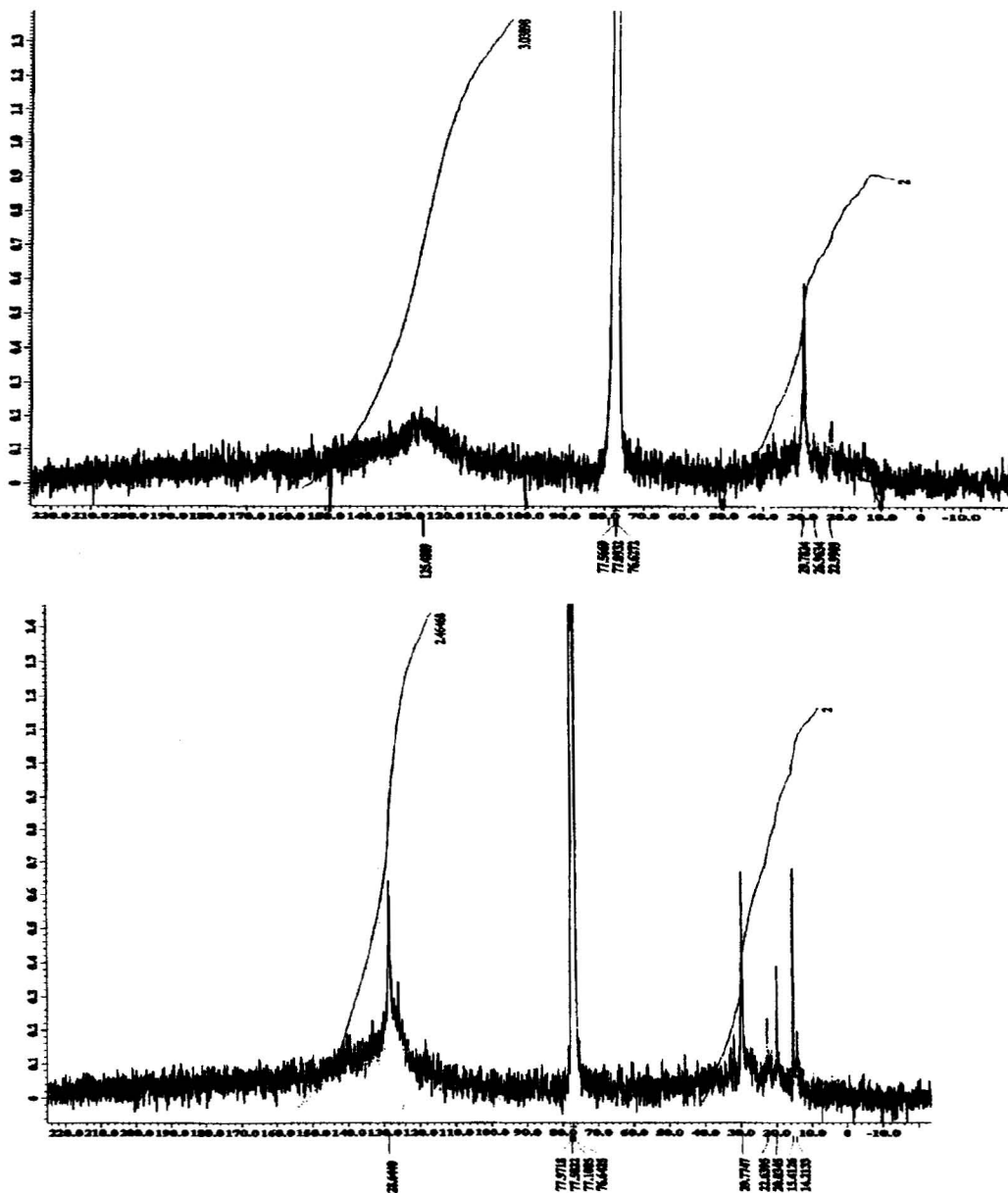


**Figure 2.**  $^{13}\text{C}$  NMR spectra of fractions A1 (top) and A2 (bottom). In  $\text{CD}_2\text{Cl}_2$ , room temperature.

**Table 4. Comparison of Structural Features of Models with Experimental Results<sup>a</sup>**

sample	H/C	C	H	DBE	$M_n$	$f_C$	$f_H$	$f_o$
fraction A1	0.92	70 <sup>b</sup>	64 <sup>b</sup>	55.8	970 <sup>c</sup>	63	8.1	46
model A1	0.89	75	67	56.8	1030	62.6	10.66	31
fraction A2	1.02	70 <sup>b</sup>	72 <sup>b</sup>	50	970	55	22	39
model A2	1.04	70	73	49	976	55.7	21.9	30

<sup>a</sup> To help comparison, some results in Tables 1 and 2 are reproduced here. <sup>b</sup> Adjusted to H/C and  $M_n = 970$ , for comparison. <sup>c</sup> Value  $M_n$  of A2 (Table 2) was also assumed for A1.

simple compounds.<sup>22</sup> This comparison is shown in Figure 4 for simple alkanes and other hydrocarbons. The sixteen points in Figure 4 were fitted to eq 5.

$$\delta_c = (1.418 \pm 0.052)\delta_o - (3.703 \pm 0.44) \quad (5)$$

Here  $\delta_c$  and  $\delta_o$  are the calculated and observed  $\delta$ , respectively.

In these calculations molecular volume were taken from the literature.<sup>22</sup> For all alkanes but dodecane,  $\Delta E$  was obtained from simple co-facial dimers formed by all trans conformers. Conformation of dodecane was adjusted to conform to the general fitting. For other compounds,  $\Delta E$  values for trimer were used because those for dimers were too low. In all cases but benzene and naphthalene, where co-facial superposition was used, molecular superposition was adjusted to reproduce the experimental  $\delta$  as closely as possible.

It should be mentioned that both  $f_H$  and  $f_C$  values of fractions A1 and A2 do not add up to the corresponding

**Table 5. Solubility Parameter and Other Properties Calculated for Models and Aggregates**

model	$-\Delta E_D^a$ (Kcal mol <sup>-1</sup> )	$-\Delta E_T^b$ (Kcal mol <sup>-1</sup> )	$V$ (cc mol <sup>-1</sup> )	$\rho$ (g cc <sup>-1</sup> )	$\delta$ (cal <sup>1/2</sup> mol <sup>-1/2</sup> cc <sup>-3/2</sup> )
M1	57	112	1008	1.02	10.52
M2	36	74	1026	0.95	8.66
2M1+M2 <sup>c</sup>		89	1017 <sup>d</sup>	0.99 <sup>d</sup>	9.37

<sup>a</sup> MM energy for dimer formation. <sup>b</sup> MM energy for trimer formation. <sup>c</sup> Intercalation of one M2 molecule Between two M1 molecules was used. <sup>d</sup> Simple average volume and  $M_w$  were used.

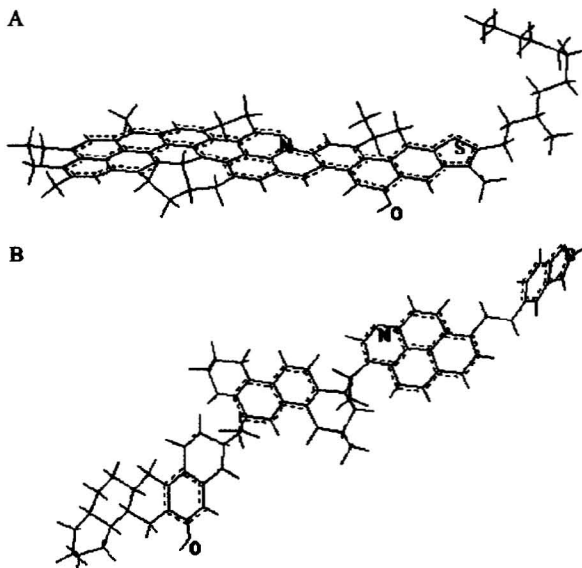


**Figure 3.** Molecular mechanics models M1 (a) and M2 (b) used to represent fractions A1 and A2, respectively.

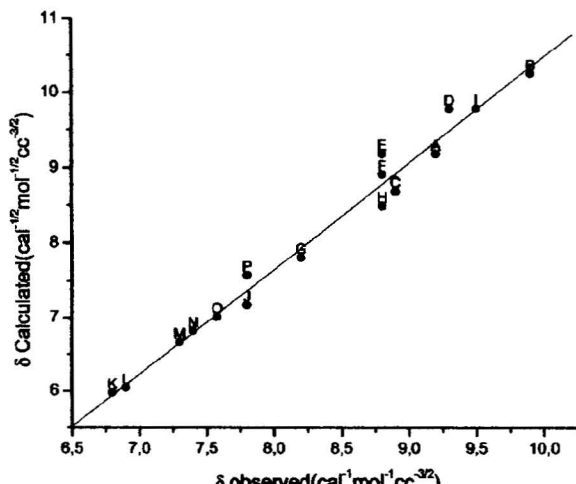


**Figure 4.** Plot of calculated against observed<sup>22</sup> solubility parameters for the following compounds: A, benzene; B, naphthalene; C, toluene; D, styrene; E, o-xylene; F, ethylbenzene; G, cyclohexane; H, decaline; I, tetrahydrodecaline; J, methylcyclohexane; K, n-butane; L, n-pentane; M, n-hexane; N, n-heptane; O, n-octane; P, n-dodecane.

values of asphaltenes (see Table 2). This appears to be due to solute–solute interactions that affect signals to some extent. As far as the present paper is concerned, we are interested *only* in the relative values of these  $f_H$  and  $f_C$  parameters for A1 and A2. Thus, whatever the reason for this anomaly, it has no bearing on the main topics of the present paper.

## Discussion

Interesting structural considerations could be made when the measured values of  $f_H$ ,  $f_C$ , and  $f_a$  are combined. Thus, low value of  $f_H$  and high values of  $f_a$  and  $f_C$  show extensive substitution of peripheral aromatic carbons in A1 and strongly suggest extensive aromatic ring fusion. We have assumed that this is the result of aromatic ring fusion with each other and with naphthenic rings. This lead us to propose model M1 for A1, where the rigid and flat core of fused PANU is the prevalent structural feature. Examination of models suggests arguments to discard the obvious general alternative, which would be to make these substitutions with methyl groups or aliphatic chains. As any molecular model would show, this entails the placement of too many bulky groups near to each other, thus leading to unacceptable overcrowding and molecular twisting.

Contrary to A1, A2 has a high  $f_a^H$  showing lower substitution of peripheral aromatic carbons and lower aromatic ring fusion. This combined with the equally high  $f_a$  and  $f_C$  led us to propose model M2 for A2.

Comparison of the experimental results with these models is shown in Table 4. The comparison is good enough for the purpose of suggesting a plausible general structural difference between fractions A1 and A2, this being the rigid and flat core in A1 versus the flexible M2 model where PANU are joined through aliphatic chains. Thus, from a qualitative point of view, one could expect that a material represented by model M2 would have a much higher solubility than the other represented by M1.

For the purpose of obtaining semi-quantitative results, we have used the solubility parameter theory. As is very well-known, this theory could now be applied, at least experimentally, to substances and mixtures of any kind.<sup>25</sup> According to this, solubility parameter is defined by the equation below:

$$\delta = \left( \frac{E}{V} \right)^{1/2} \quad (6)$$

Here,  $E$  is the vaporization energy. Using the procedure described above, we have related the experimental and theoretical  $\delta$  for several simple compounds. Since the experimental  $V$  was used in these calculations, the values of  $E$  and  $\Delta E_{MM}$  are the ones actually compared in Figure 4. Value  $-\Delta E_{MM}$  could be defined as the energy required to vaporize the trimer or dimer under vacuum at 0 K. Accordingly, it is not expected to be equal to  $E$ . However, the good fitting found in Figure 4 strongly

(23) Acevedo, S.; Ranaudo, M. A.; Pereira, J. C.; Castillo, J.; Fernández, A.; Perez, P.; Caetano, M. *Fuel* **1999**, *78*, 997–1003.

(24) Norinaga, K.; Wargardalam, S.; Takasugi, S.; Iino, M.; Matsukawa, S. *Energy Fuels* **2001**, *15*, 1317–1318.

(25) Hansen, C. M. *Hansen Solubility Parameters. A User Handbook*; CRC Press: Boca Raton, FL, 2000.

suggests that these quantities are related and can be used in a comparative way.

This we did for M1 and M2, and the results for  $\delta$  are shown in Table 5 along with the calculated  $V$ ,  $\rho$ , and energy values. In view of their large difference in solubility, the relatively large calculated difference in  $\delta$  is expected.

As shown above, neither  $M_w$  nor heteroatom content plays any significant role in the solubility difference between A1 and A2. This strongly suggests that the main factor in determining asphaltene solubility would be the way PANU are assembled. Above we have illustrated, in a simple (but consistent way), an example where a large solubility difference could be expected. Certainly there are others, and the extreme complexity of asphaltene precludes a more complete analysis here.

However, we believe that beyond any specific details, and in view of the high aromatic content and high  $M_w$  of asphaltenes, flexible structures, such as the one for M2, are the ones expected to have high solubility in toluene.

When measured by VPO, A1 yields a  $M_n$  higher than the one for A2 (see Table 3). However, when measured by LDMS and SEC,  $M_n$  for A1 and A2 afforded similar or equal values. Also, the VPO value corresponding to their natural mixture (asphaltenes) is close to the one for A2 (see Table 3). This strongly suggests that the high VPO value found for A1 is due to aggregation and that the presence of A2 precludes aggregate formation. In view of the solubility behavior of asphaltenes (soluble in toluene) and A1 (insoluble in toluene), the above  $M_w$  phenomena are not surprising.

These phenomena could be accounted for in terms of energy interactions in the solid mixture. According to the  $-\Delta E_D$ ,  $-\Delta E_T$ , and  $\delta$  in Table 5, we could expect that intercalation of A2 between two A1 (fourth row in Table 5) would enhance its solubility. Once in solution, future events depend on conditions. For instance, in appropriate solvents of high  $\delta$  (for nitrobenzene  $\delta = 10^{22}$ ), high temperature, and relatively low concentration, the present VPO information suggests that strong solvation of A1, rather than dispersion in solution by A2, is the prevalent mechanism. For dispersion, some kind of interaction between fractions should exist in solution and this would yield a higher than found  $M_n$  value.

For solvents where  $\delta$  is not high enough, such as aromatics ( $\delta < 9.5^{22}$ ), A1 aggregates would form, even at very low concentrations.<sup>23,24</sup> Adsorption of A2 on these aggregates would prevent growing beyond colloidal size, resulting in the usual high solubility of asphaltene in these solvents.

According to the MM energies (see Table 5), one could generally expect, on thermodynamic grounds, that interaction energy between two colloidal particles, being of the A1–A1 type, should not be avoided by the weaker A1–A2 interaction. This probably means that dispersion of A1 by A2 is a kinetic effect, where the activation energy for desorption of A2 is the stabilization factor.

## Conclusions

Use of the PNP method allowed the separation of asphaltenes in fractions A1 and A2 characterized by very significant structural differences and similarities. These lead us to propose model structures for them, which were consistent with experiment and with solubility behavior for them and their natural mixture (asphaltenes). The rigid and flat structural core, formed by extensive fusion of aromatic and naphthenic rings leading to a single PANU, employed to model A1 and the flexible model used for A2, represented by several smaller PANU connected by aliphatic chains, are the most distinct feature of these models. The solubility parameters calculated for these models were in keeping with observed solubility. The present experimental and theoretical results were used to propose solubility and molecular weight phenomena of asphaltenes.

**Acknowledgment.** We thank Drs. Jonathan Mathews and Daniel Jones from The Pennsylvania State University for the LDMS spectra. The financial support of FONACIT (Grants G97000722 and 97004022) is gratefully acknowledged. We also thank the technical support of Lic. Betilde Segovia.

## Nomenclature

- A1 = low-soluble fraction of asphaltene
- A2 = high-soluble fraction of asphaltene
- Ar<sup>-</sup> = aromatic ring
- $\delta$  = solubility parameter
- DBE = double-bond equivalent
- $E$ ,  $\Delta E$  = energy values
- $f_a$  = percentage of H<sub>a</sub> hydrogens
- $f_c$  = carbon aromaticity; equal to percentage of aromatic carbons
- $f_H$  = hydrogen aromaticity; equal to percentage of aromatic hydrogens
- H<sub>a</sub> = hydrogen bonded to aliphatic carbon  $\alpha$  to an aromatic carbon such as Ar–CH $\alpha$
- H/C = atomic hydrogen-to-carbon ratio
- LDMS = laser desorption mass spectroscopy
- MM = molecular mechanics method for calculation of optimal geometries and energies
- $M_n$  = number average molecular weight
- $M_w$  = molecular weight
- N/C = nitrogen-to-carbon ratio
- O/C = oxygen-to-carbon ratio
- PANU = polycyclic aromatic and naphthenic units present in asphaltenes
- PNP = *para*-nitrophenol
- PNP method = method for fractionation of asphaltenes in fractions A1 and A2
- $\rho$  = density
- S/C = sulfur-to-carbon ratio
- SEC = size-exclusion chromatography
- THF = tetrahydrofuran
- TLC-FID = thin-layer chromatography with a flame ionization detector
- $V$  = molar volume
- VPO = vapor pressure osmometry

EF030065Y